MODELING OF TRAPPED PLAMA MODE OSCILIATIONS IN AP$^+$ N – N$^+$ SILICON DIODE

BY

C.O.G. OBAH

Department of Electrical & electronic Engineering

University of Nigeria, Nsukka, Nigeria.

ABSTRACT

This paper proposes an approach for obtaining a relatively simple set of equations which apply to the description of TRAPATT phenomenon and applies it to model trapped-plasma mode oscillations in a p^+ n – n^+ silicon diode.

Typical voltage, conduction current, electric field and carrier charge wave-forms are presented for a square wave of drive current. The diffusion transport phenomenon is shown to affect the diode operating characteristics. The subperiods of the diode voltage and conduction current are found to be useful parameters in dilineating the diode operating frequency limits.

The influence of the diode physical parameters and the effects of the package circuit parasitic on the diode performance are explored, and curves for practical design presented. The predicted RF performance shows good agreement with experimental measurement for a typical L-band TRAPATT oscillator.

NOTATION

I_T	eternal drive current
I_{pk}, I_{nk}	hole and electron current crossing boundary K
Δ_{xk}	width of Kth lump
P_{Bk} , n_{Bk}	hole and electron Kth boundary densities
P_k, n_k	average hole and electron densities in lump K
A_D	diode area
q	electronic charge
Q_{pk} , Q_{nk}	magnitude of total hole and electron charges
α_{pk} , α_{nk}	hole and electron ionization rates at Kth boundaries
υ_{pk} , υ_{nk}	hole and electron carrier velocities at Kth boundaries
υ_{sp}, υ_{sn}	hole and electron saturation velocities
N_a, N_d	fixed ionized acceptor and donor impurities
I_{ps}, I_{ns}	hole and electron reverse saturation current components
I_S	total reverse saturation current
N_D	net doping concentration
μ_p, μ_n	hole and electron mobilities
D_p , D_n	hole and electron diffusion constants
K	Boltzman constant
T	absolute temperature
E	total diode electric field
E_K	electric field at boundary K
I_C	diode conduction current
J_N	drive current factor
E_B	diode breakdown field
Q	time derivative of Q
E	time derivative of E
V_D	diode terminal voltage
V_B	diode breakdown voltage
ω	diode active (avalanche) region width
ε	permittivity of doped semi conductor

R_p package series resistance
L_p effective package series inductance
C_p package shunt capacitace

The ionization rates are assumed to be of the form (1) – (2) for silicon.

$\alpha_p = 2.25 \times 10^7 \exp\left(\frac{-3.26\times10^6}{E}\right)$ for holes,

$\alpha_n = 3.80 \times 10^6 \exp\left(\frac{-1.75\times10^6}{E}\right)$ for electrons,

while the carrier velocities are taken as

$\upsilon_p = \upsilon_{sp} (1 - \exp(-\gamma_p E)$,

$\upsilon_{sp} = 7 X 10^6$ cm/sec

$\upsilon_n = \upsilon_{sn} (1 - \exp(-\gamma_n E))$,

$\upsilon_{sn} = 10^7$ cm/sec

where $\gamma_{p'}$, γ_n are hole and electron velocity constants, (1.49 x 10^{-4}cm/v, 0.85 x 10^{-4} cm/v for silicon), determined by curve fitting the function to the experimental data (3) – (4).

INTRODUCTION

Trapped plasma mode avalanche semiconductor devices, commonly called TRAPATT diodes, are well known for achieving reliable high output powers (up to 1 KW or more in pulsed mode) and high efficiencies (up to 60 percent) when operating as single diode chips [5] – [8]. These unique capabilities make the devices potentially useful for many applications in military and commercial communication systems such as fuses for missile guidance and anti-aircraft gun control, high data rate FM transmitters, aircraft landing systems and high power satellite transponder systems [8]- [12]. The expected rapid advances in TRAPATT technology development, however, have not yet been fully realized due first to the fact that the complex nature of the device intrinsic behavior is not yet well understood, and secondly to the fact that there is incomplete knowledge of the complex TRAPATT diode – external circuit interaction involved in the operation of the device in a practical RF circuit. If the potential systems applications of these devices are to be fully exploited, there is, therefore, a need for continued efforts towards the better understanding of the intrinsic behaviour of the devices, the critical factors affecting their efficient operation and ways of optimally incorporating them in RF circuits.

The design of practical TRAPATT circuits calls for a modeling approach suitable for both the complete diode and diode-external circuit interaction analysis. Published models and modeling techniques applicable to trapped plasma mode phenomena [13] – [16] are largely device – physics oriented. Although they employ actual device equations in their analyses, they are in general, either too costly or too restrictive for design purposes, particularly where the device external circuit interaction is to be studied. Existing circuit– design oriented models [17] -[18], on the other hand, require a priori knowledge of various parameters and employ little device-physics. Their usefulness is further limited where performance characteristics must be explored as functions of device structures and materials.

This paper describes a “compromise” modeling approach suitable for the analysis of both the actual TRAPATT device physics and the device – external circuit interaction. The only diode characteristics required for simulation are the active region width, diode area, breakdown voltage and doping profile, and these are easily measurable quantities for a given diode structure. The physical mechanisms associated with trapped plasma mode oscillations in P^+ –N–N^+ silicon diodes are presented. Parametric studies are also carried out to explore the effects of diode physical parameters and package circuit parasitics on the diode performance. The useful operating frequency limits of trapped plasma mode oscillations are dilineated. The actual effects of diffusion transport phenomena on the diode performance are studied.

2.0 FORMULATION OF THE PHYSICAL MODEL

2.1 THE MODELING TECHNIQUE

The model, for a given TRAPPATT diode structure is based on distributed avalanching phenomena throughout the whole diode active region. It is obtained by dividing the diode active region into cells or lumps and applying to each lump the general partial differential equations governing the behaviour of carriers and electric fields in an avalanching semi-conductor chip. The equations of interest are the one-dimensional partial differential equations for the generation, diffusion and drift of holes and electrons as well as poison's and the conservation of current equation. By assuming uniform spatial variation of carrier charges and linear variation of electric fields in each cell, a relatively simple time domain device-physics model, consisting of a set of coupled first – order differential equations is obtained. The model is a flexible one, accommodating any arbitrary doping profile, different ionization rates for holes and electrons, unsaturated and unequal carrier velocities, unequal diffusion constraints, and any modifications to reflect refinements in the user's requirement such as the number of lumps. Thus, for specified diode parameters, namely area (A_D) , active region width (W), breakdown voltage (V_B) and doping profile, and given external current drive (I_T), the model predicts whether or not trapped plasma mode oscillations are possible.

One of the major advantages of the technique is that, since the diode package and the external circuit may also be described in time domain, a simple simultaneous solution to the complete device – external circuit complex may be obtained. Therefore any circuit instabilities may be recognized and corrected with minimum computation while the circuit element values necessary to sustain efficient trapped plasma mode oscillations at the diode are predicted. Thus circuit optimization is rapid. The economical nature of the present method is further enhanced by the fact that a small number of cells (lumps) give reasonably accurate results.

2.2 ANALYSIS

Consider a general P^+–N–N^+ TRAPATT diode with the avalanche active region, of constant width W, partitioned into L–cells or lumps as shown in Fig.1.

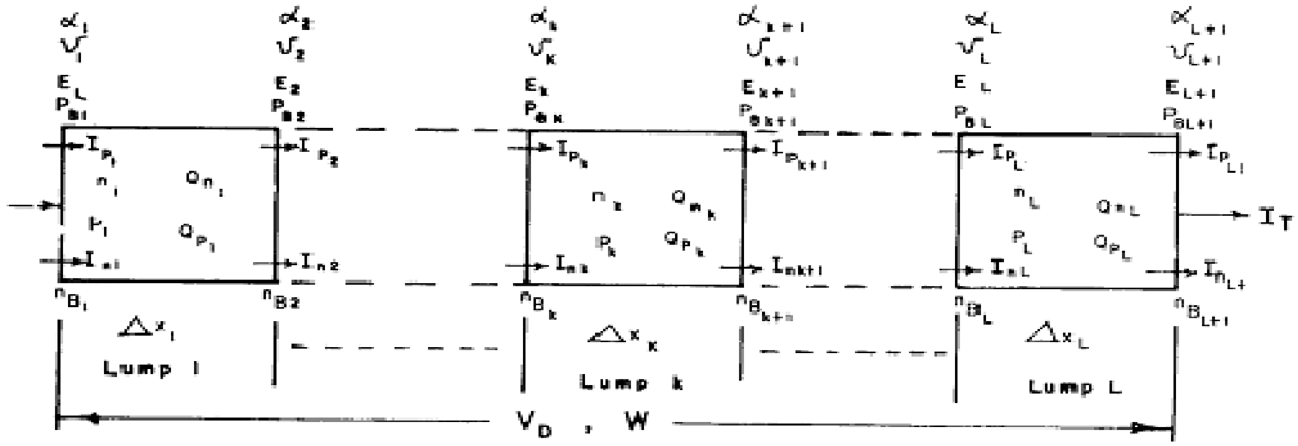

Fig. 1: Partitioned active region width showing lump variables

For an abrupt junction device and equal lump width condition, the basic general equations in one dimension governing the behaiour of carriers and electric fields become for the Kth lump.

(a) Continuity Equation

$$\dot{Q}_{nk} = \Delta I_{nk} + \alpha_{nk} \cup Q_{nk} + \alpha_{pk} \cup_{pk} Q_{pk} \text{ , for electrons} \quad (1)$$

$$\dot{Q}_{pk} = -\Delta I_{nk} + \alpha_{nk} \cup_{nk} Q_{nk} + \alpha_{pk} \cup_{pk} Q_{pk} \text{ , for holes}$$

$$\text{Where}\Delta I_k = (I_{k+1} - I_k), : \frac{\partial}{\partial x} \to \frac{\Delta}{\Delta x}$$

(b) Poisson's Equation

$$Q_{pk} = Q_{nk} + \varepsilon A_D (E_{k+1} - E_k) - Q_D \quad (2)$$

Where $Q_D = Q_{nk} - Q_{Nd} = qA_D(N_d - N_a)\Delta x$

And from the conservation of current equation we obtain

$$\dot{E}_k = \frac{I_T}{\varepsilon A_D} - \frac{I_{nk}}{\varepsilon A_D} - \frac{I_{pk}}{\varepsilon A_D} \quad (3)$$

Where $I_{nk} = I_{on_k} + I_{nD_k} + I_{ns}$, for electrons .... (4)

$I_{on_k} = (qA_D \vartheta_{nk} n_{Bk})$ kthboundary electron drift current

$I_{nD_k} = \left(qA_D D_n \left\{\frac{n_{k+1} - n_k}{\Delta x}\right\}\right)$ kth boundary electron diffusion current.

Similar definitions apply for the hole current I_{pk}.

Since Q_n, Q_p are coupled through equation (2), we can eliminate either one by substitution. Combining equation (2) and (1) yields:

$$\dot{Q}_{nk} = \Delta I_{nk} + (\alpha_{nk} \upsilon_{nk} + \alpha_{pk} \upsilon_{pk}) Q_{nk} + \varepsilon A_D \alpha_{pk} \upsilon_{pk} (E_{k+1} - E_k) - \alpha_{pk} \upsilon_{pk} Q_D \quad (5)$$

The average lump carrier densities (Fig. 1) are given by

$$P_k = \frac{P_{Bk}+P_{Bk+1}}{2} \quad \text{for holes} \tag{6}$$

$$n_k = \frac{n_{bk}+n_{Bk+1}}{2} \quad \text{for electrons}$$

Since $I_{nk} = I_{on_k} + I_{nD_k} + I_{ns}$; $I_{pk} = I_{op_k} + I_{pD_k} + I_{ps}$ (7)

and I_{ns}, I_{ps} constant.

Then

$$\Delta I_{nk} = I_{nk+1} - I_{nk} = \Delta I_{on_k} + \Delta I_{nD_k};\ \Delta I_{pk} = \Delta I_{op_k} + \Delta I_{pD_k} = I_{pk+1} - I_{pk} \quad (7)$$

Equation (6) is used to evaluate the boundary carrier (hole and electron) densities and hence the boundary carrier drift and diffusion currents to yield boundary hole and electron currents for L-lumps as:

$$I_{pk} = \frac{2\upsilon_{pk}}{\Delta x}\sum_{m=k}^{L+1}(-1)^{m-k}\, Q_{pk} - \frac{D_p}{(\Delta x)^2}\{Q_{pk+1} - Q_{pk}\} + I_{ps}, (k = 1,2, \dots, L+1) \dots (8)$$

$$I_{nk} = \frac{2\upsilon_{nk}}{\Delta x}\sum_{m=k}^{L+1}(-1)^{k-m+1}Q_{nm} + \frac{D_n}{(\Delta x)^2}(Q_{nk+1} - Q_{nk}) + I_{ns}, (K = 1,2, \dots, L+1) \dots (9)$$

Putting equation (9) in equation (7) gives for electrons:

$$\Delta I_{nk} = I_{nk+1} - I_{nk}$$

$$= \frac{2}{\Delta x}(\upsilon_{nk+1} + \upsilon_{nk})\sum_{m=1}^{k-1}(-1)^m Q_{nk-m} + \left(\frac{2\upsilon_{nk+1}}{\Delta x} + \frac{D_n}{(\Delta x)^2}\right)Q_{nk}$$

$$-\frac{D_n}{(\Delta x)^2}(2Q_{nk+1} - Q_{nk+2}) \quad \dots \quad \dots \quad (10)$$

Equation (10) in equation (5) yields:

$$\dot{Q}_{nk} = \frac{2}{\Delta x}(\upsilon_{nk+1} + \upsilon_{nk})\sum_{m=1}^{k-1}(-1)^m Q_{nk-m} + \left(\alpha_{nk}\upsilon_{nk} + \alpha_{pk}\upsilon_{pk} + \frac{D_n}{(\Delta x)^2} + \frac{2\upsilon_{nk+1}}{\Delta x}\right)Q_{nk}$$
$$-\frac{D_n}{(\Delta x)^2}(2Q_{nk+1} - Q_{nk+2}) + \varepsilon A_D\alpha_{pk}\upsilon_{pk}(E_{k+1} - E_k) - \alpha_{pk}\upsilon_{pk}Q_D \quad \ldots (11)$$

Equation (8) and (9) in equation (3) gives:

$$\dot{E}_k = \frac{-2\upsilon_{nk}}{\varepsilon A_D \Delta x}\sum_{m=1}^{k-1}(-1)^{k-m+1}Q_{nm} + \frac{D_n}{\varepsilon A_D(\Delta x)^2}(Q_{nk} - Q_{nk+1})$$
$$-\frac{2\upsilon_{pk}}{\varepsilon A_D \Delta x}\sum_{m=k}^{L}(-1)^{m-k}Q_{nm}\frac{D_p}{\varepsilon A_D(\Delta x)^2}(Q_{nk} - Q_{nk+1})$$
$$-\frac{2\upsilon_{pk}}{\Delta x}\sum_{m=k}^{L}(-1)^{m-k}(E_{m+1} - E_m) + \frac{D_p}{(\Delta x)^2}(E_k - 2E_{k+1} + E_{k+2}) + \frac{I_T - I_s}{\varepsilon A_D}$$
$$+\frac{2\upsilon_{pk}}{\varepsilon A_D \Delta x}\sum_{m=k}^{L}(-1)^{m-k}Q_D \ldots\ldots\ldots\ldots\ldots\ldots\ldots\ldots\ldots (12)$$

Equations (11) and (12) are the required state-equations describing the TRAPATT diode internal behaviour for an abrupt junction structure with equal width partitioning. For an Arbitrary Doping profile, e.g. graded junction, Unequal lump width partitioning must be used. In this case Δx and Q_D are replaced by Δx_K and Q_{Dk} respectively.

In the above equations (11) and (12) , it is seen that the diode active region behaviour is completely characterized by a set of (2L+1) first-order differential equations involving L equations for the lump charge derivatives and (L+1) equations for the lump boundary electric field derivatives.

The voltage V_D, across the active region is given by:

$$V_D = \frac{1}{2}\Delta x\sum_{k=2}^{L+1}(E_{k-1} + E_k)$$

for abrupt junction structure;

$$V_D = \frac{1}{2}\sum_{k=2}^{L+1}(E_{k-2} + E_k)\,\Delta x_{k-1}$$

, for arbitrary doping structure; … … … (13)

The diode conduction current is simply:

$I_c = I_T - A_D\dot{E}$ … … … … … … … (14)

Thus for a given diode and external drive current, I_T, the diode voltage and current wave forms are easily obtained.

3.0 DIODE INTRINSIC BEHAVIOUR

3.1 NUMERICAL CALCULATIONS

The model system of equations is solved on a digital computer. To carry out simulation, the initial conditions are determined by assuming a small and constant value of current flowing through the diode reverse biased at breakdown, and setting all the time derivatives to zero. For a large step in drive current, the time taken for the diode terminal voltage to recover to its breakdown value after it has collapsed to a very low value gives half the oscillation period and thus the duration of the external (applied) current drive. This procedure removes(18) the arbitrary choice of current duration employed by the existing trapped plasma mode analyses [13, 14, 17, 18]. The required number of lumps, L, to realistically model the TRAPATT phenomena for a given width is determined from extensive tests for convergence and accuracy. Fourier analysis of the applied current and the corresponding diode voltage yields the diode RF power and dc – Rf conversion efficiency.

3.2 INTRINSIC OPERATING CHARACTERISTICS AND DIFFUSION CURRENT EFFECTS

Fig. 2 and 3 show the typical voltage, lump electron charge and electric fields for a general P^+ - N - N^+ abrupt junction diode (A_D = 1.55 x 10^{-4} cm^2, V_B = 90V, W = 3μm and doping density N_D = 1.75 x 10^{15} cm^{-3}) for specified drive current factor, J_N = (I_T/2 .q. A_D.N_D . V_{sn}) with and without the inclusion of diffusion current effects. The electric fields, Fig. 3, are plotted at arbitrary increasing voltage time

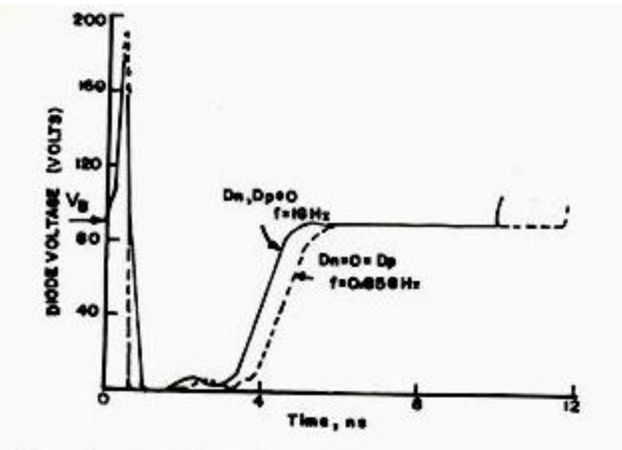

Fig.2(a): Effect of diffusion transport phenomenon on voltage.

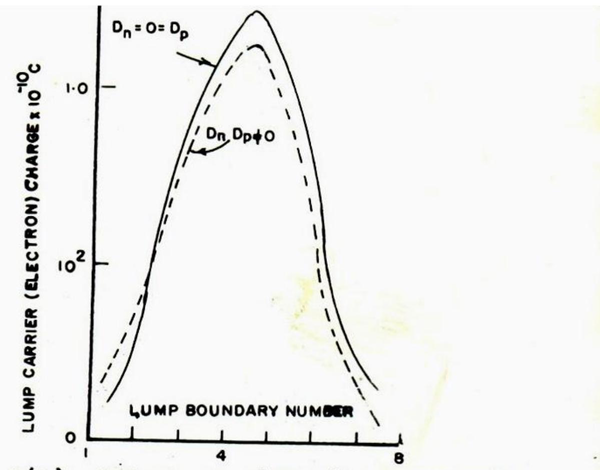

Fig.2(b): Effect of diffusion transport phenomenon on lump charge (J_N = 2).

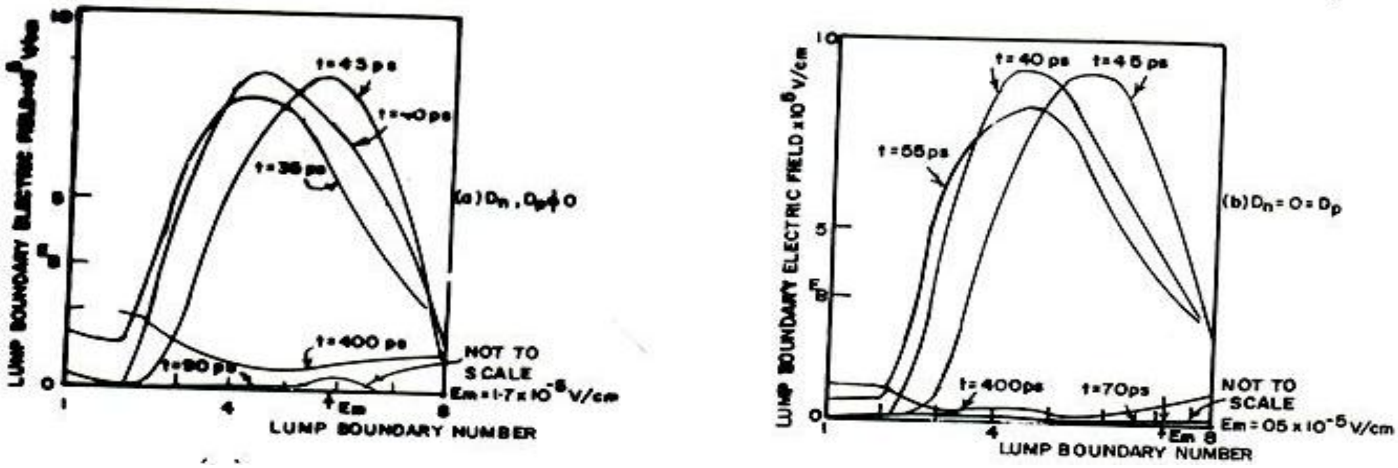

Fig. 3: Lump boundary fields at selected voltage time frames. (J_N=2) (a) with (b) without diffusion effects.

frames corresponding to: 5ps before maximum diode voltage, at voltage maximum, 5ps later, at voltage minimum and finally at 400ps from t (time) = 0. The lump electron charge is plotted at the time of maximum diode voltage. The graphs exhibit all the salient features of the existing trapped plasma mode oscillations phenomena [13 ,14] namely: both the diode voltage, Fig. 3, peak simultaneously, and the fields throughout the diode collapse to near zero as the voltage reaches its minimum value; as the region of the field above the breakdown value, E_B, (traveling avalanche zone) shifts to the right across the diode, the fields in its wake are increasingly depressed while those in its immediate front are being rapidly increased. But additional features not previously reported in the literature are also discernable. These features included the influence of diffusion current effects and the varying width of the traveling avalanche zone. Inclusion of diffusion current effects (D_n = 0. D_p = 0) is seen to reduce the peak voltage (and field) reached at the onset of the total voltage collapse, to increase the oscillation frequency to reduce the duration of the trapped plasma, and finally to reduce the traveling avalanche zone obtained. These results strongly suggest that careful control of diffusion current parameters during the TRAPATT diode fabrication is essential.

3.3 RESPONSE CHARACTERISTICS VARIATION WITH APPLIED CURRENT

Fig. 4 shows the lump carrier charg at the various times of voltage minimum and maximum for varying drive current factor, J_N . The shifting of the center of the lump carrier charge further away from the metallurgical junction as J_N increases, indicates a broader effective avalanching process with increase in current density. The effective width, defined as measured to $\frac{L\pm}{e}$ = 37% of the peak lump carrier charge at the time of voltage maximum, is seen to be an appreciable portion of the total diode active region width. These results suggest the following conclusions: Although avalanching process may be taking place throughout the active

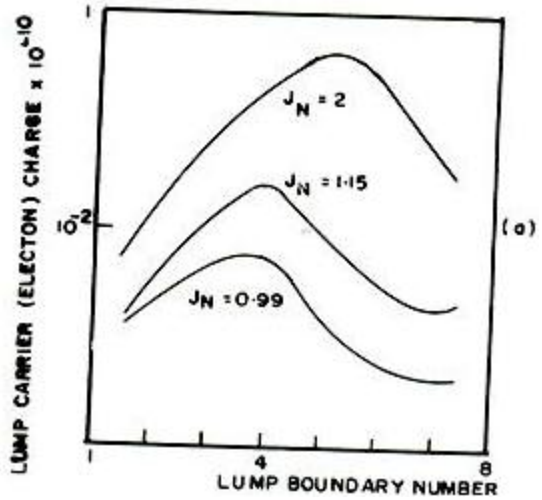

Fig. 4(a): Lump charges for varying bias current at voltage minimum

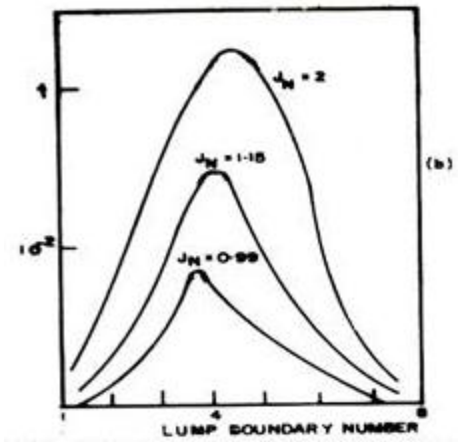

Fig. 4(b): Lump charges for varying bias current at voltage maximum

region width for terminal current levels higher than the critical value, the effective avalanching width for a given TRAPATT diode structure is an increasing function of the current density; thus in an actual TRAPATT circuit, the effective avalanching width rather than the nominal active region width could be an important frequency controlling parameter. This observation partly explains why the reported empirical design criterion [14] relating the avalanche region width W in microns to optimum operating frequency. f_{opt} in gigahertz, f_{opt} = 7/W, has been difficult to obtain in practice for known TRAPTT structure.

The conduction current variation is shown in Fig. 5. Note that the current exhibits a pronounced peak (avalanche conduction state) and a plateau (extraction conduction state), and the current widths diminish with decreased in applied current. This implies the reduction of power generation capability with decrease in current as is expected in practice. Fig. 6 shows the possible limits of the diode model response with J_N.

The voltage response indicates that for J_N = 0.87, little or no trapped plasma characteristics are evident and the IMPATT mode may predominate, while for J_N = 6.00, the voltage returns to its breakdown values more than once in a cycle. This latter case is characterized by a large spike in voltage, faster rise and fall times, and is said to be exhibiting heavy plasma characteristics. The computed efficiency for this case is 21% showing that, although

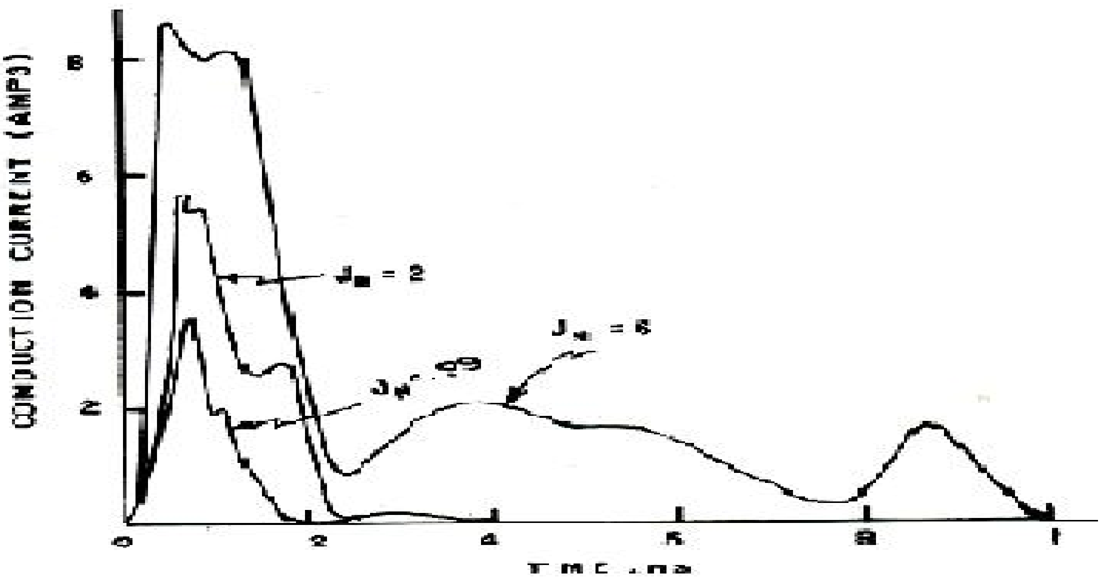

Fig. 5: Diode conduction current with bias current

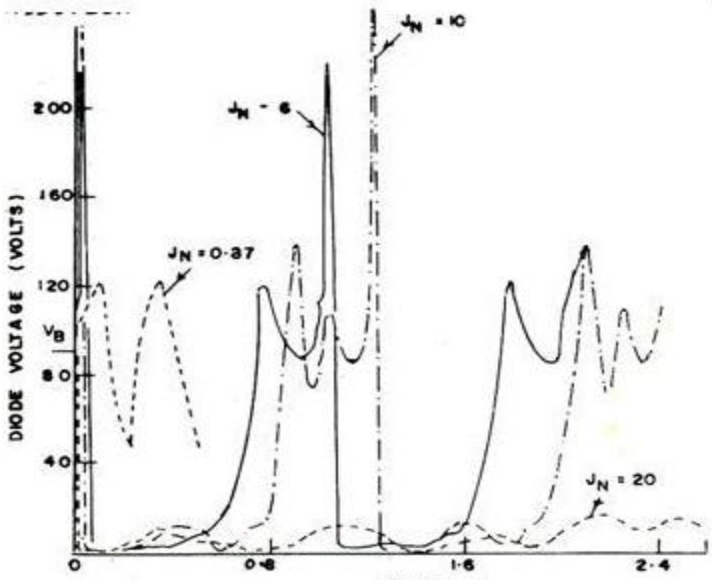

Fig.6: Possible diode model voltage response limits.

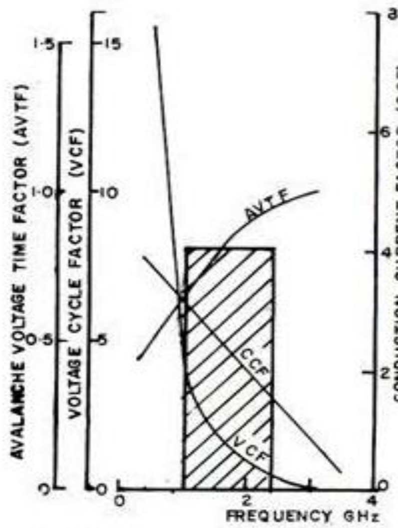

Fig.7: Frequency limits for useful TRAPATT operation.

the diode possesses higher power generating capability at high-applied current levels, it may do so at substantially reduced efficiencies. The voltage response for $J_N = 20$ shows that when the applied current exceeds a certain upper limit, the model diode is suddenly saturated with trapped – plasma. In a practical circuit, such a condition may result in the diode burn-out.

From the above results, it is evident that the frequency limits for useful trapped plasma mode oscillations of a given diode structure may by be studied by examining the subperiods of the diode response. Fig. 7 examines these frequency limits in terms of the following descriptive phrases: avalanche voltage time factor, AVTF (voltage rise time/voltage fall time), voltage cycle factor, VCF (voltage recovery period/voltage charging period), and conduction current factor, CCF, (peak avalanche current/peak extraction current.). The upper frequency limit is shown to be synonymous with low CCF, near unity AVTF and almost zero VCF. This corresponds to a spiky condition current waveform and short trapped-plasma duration condition. The lower frequency limit, on the other hand, is seen to be the diode operating condition with high CCF and VCF. This corresponds to the diode plasma formation. The optimum efficiency region of the diode (shaded portion of the diagram) lies within the frequency range for which $J_N \leq 5$ and efficiency ≤30 percent.

The results described above suggests a possible tuning criterion for diodes when embedded in actual RF circuits. The shape of the diode voltage and conduction current waveforms is related to the quality of the operational output waveforms obtained in a practical TRAPATT circuit, and is largely controlled by the circuit tuning conditions. Thus the diode should be tuned to operate in the optimum efficiency region if high quality output waveforms are desired. High quality output characteristics are, of course, highly desirable for many potential applications of TRAPATT diodes particularly pulsed radar and aircraft landing systems.

3.4. INFLUENCE OF DIODE PHYSICAL PARAMETERS

A vital information in the design and in the actual fabrication of TRAPATT diodes is the effect of the diode physical parameters on the device power capability and operating frequency. Figs. 8 and 9 are the results of some of the parametric studies on the model diode. The maximum TRAPATT frequency (Fig. 8) corresponds to the maximum

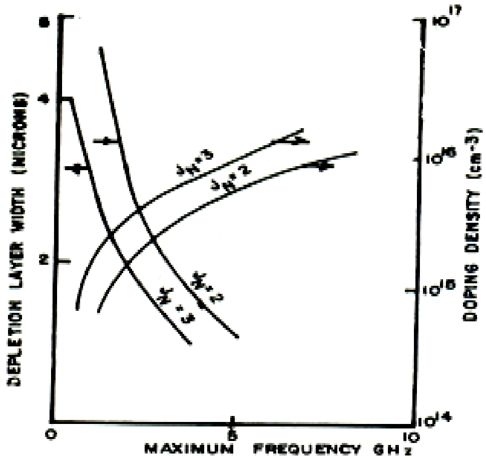

Fig.8: Operating frequency VS doping density & diode width.

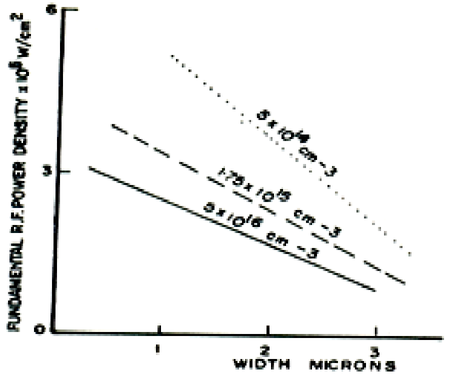

Fig.9: RF power density VS diode width.

attainable oscillation frequency for a given drive current factor. It is seen that the maximum frequency is inversely proportional to the active region width as is expected in practice. Fig. 9 shows that the RF power density is linearly related to the active region width. Above results strongly suggest that narrow P^+ - N - N^+ TRAPATT silicon diodes (W≤5 microns) would probably yield their highest RF power outputs and efficiencies when fabricated with low doping density, and that for a specified operating frequency, high doping density would require high current density to initiate trapped plasma mode oscillations.

3.5. EFFECT OF THE PACKAGE CIRCUIT PARAMETER

In addition to the careful choice of material parameters and the close process control required in the manufacture of TRAPATT diodes, careful attention must be given to the local environment surrounding the diode, namely the diode package. This is essential if the diode is to be optimally incorporated into the external RF circuit. In this section, typical effects of some of the package parasitics on the model diode performance are examined. A common packaging configuration for the diode is considered in this paper. Its equivalent circuit (Fig. 10) is obtained by assuming that the package behaves essentially as a lossy inductive element in series with the diode, together with a shunt capacitance [19], although more complicated models [20] may be considered. The package elements are represented as lumped because the physical dimensions are normally smaller (typically <0.05λ) than the wavelengths

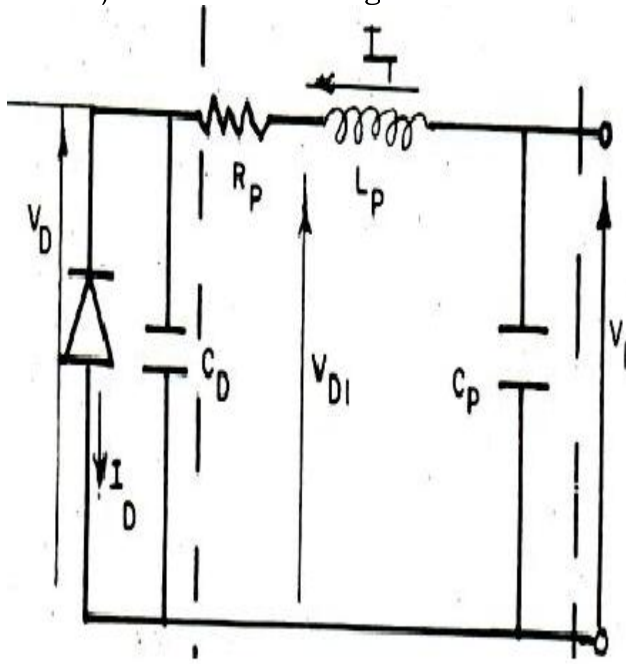

Fig. 10: Packed Diode equivalent circuit assumed

of interest. By solving the diode model equations together with the relevant package current and voltage equation ($\dot{I}_T = -I_T \frac{R_P}{L_P} + \frac{V_P - V_D}{L_P}$; $V_{D1} = V_D + I_T R_P$), the influence of R_P and L_P can be studied. Fig. 11a shows the effect of R_P on the diode voltage response. R_P is seen not to affect the diode recovery time but to reduce the trapped plasma obtained. Consequently R_P should have

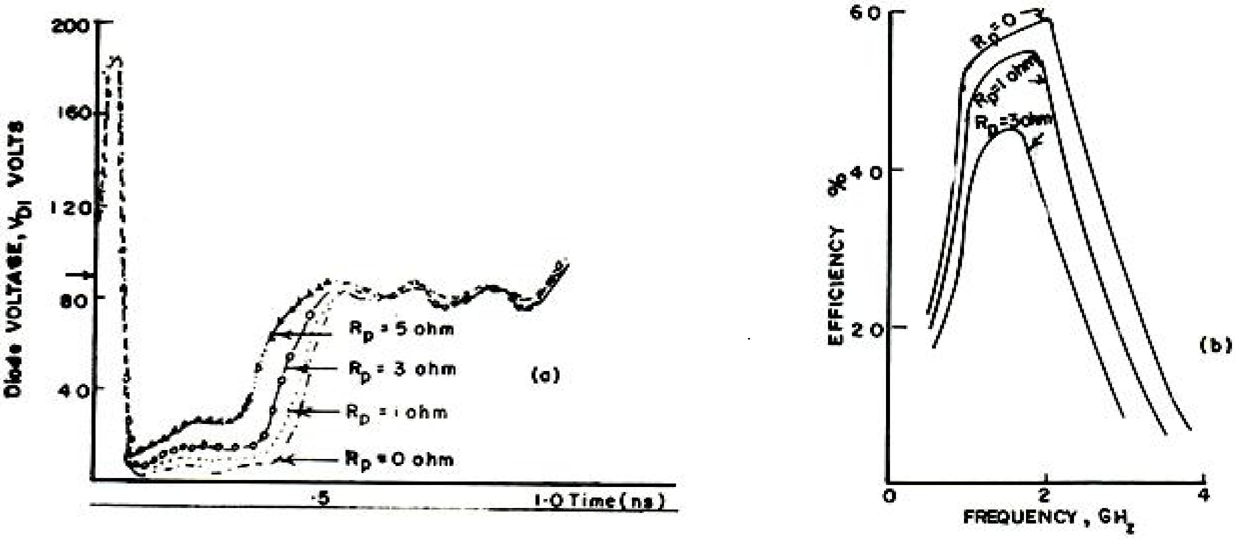

Fig.11: Computed effect of package resistance, R_p on (a) diode voltage (b) efficiency.

a strong influence on the diode efficient operation as shown in Fig. 11b. The effect of the package inductance is indicated in Fig. 12a. It is shown that large values of the package inductance (and hence inductance nearest the diode) not only excite large transients in the quiescent portion of the voltage waveform but may also cause large amplitude distortion during the high conducting state of the diode. This implies a deterioration in the diode performance and a decrease in the operating frequency. This effect is shown in Fig. 12b, which also indicates the existence of an optimum diode performance. The above results suggest the following conclusions:-

Optimum interaction – between the TRAPATT diode and the package circuit (and hence external RF circuits) requires that the trapped plasma mode oscillations originating from the device must not degrade appreciably as they pass through the diode package

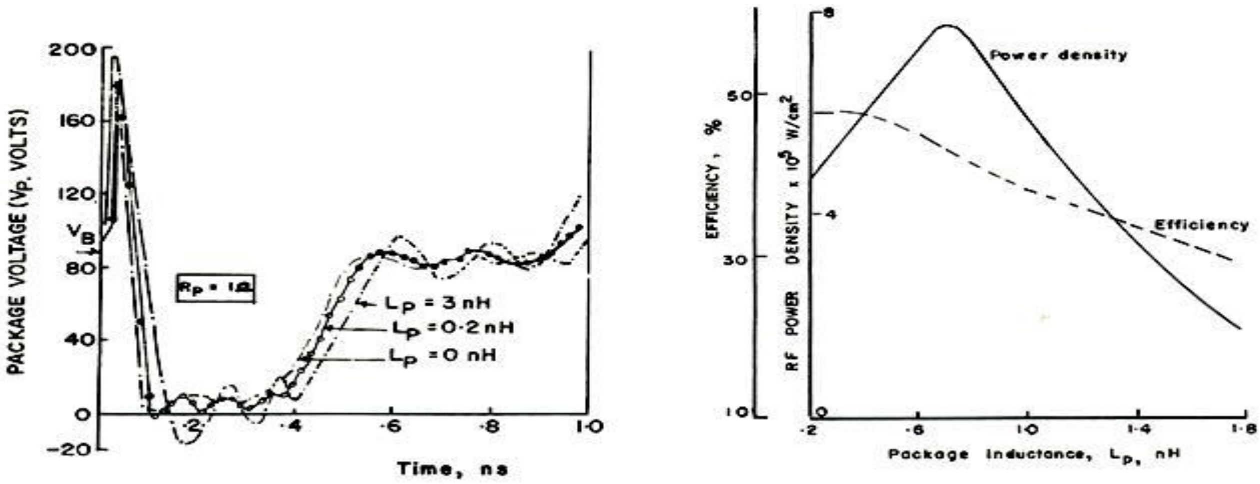

Fig.12: Computed effect of package inductance, L_p on (a) voltage response (b) diode performance.

to the external circuit, and a moderate amount of inductance in the vicinity of the diode is essential for optimum performance in a practical TRAPTT circuit.

3.6. EXPERIMENTAL RESULTS

Experimental investigations were carried out on a typical high-power L-band graded junction TRAPATT diode (Hughes Aircraft Company, Model NWA 729) using a conventional waxial TRAPATT oscillator cavity [21] employing four tuning slugs. The pertinent diode parameters are: active region width (8microns), N_D (3.4×10^{-4} cm^{-3}), V_B (200 volts), Diameter (800microns), R_P (1.5ohm), L_P (0.3 nH), C_P (0.3pF).

For each operating current level, the diode was tuned for optimum efficiency consistent with high – quality output waveforms in order to reduce detected RF leading-edge Jitter and obtain relatively noise free and stable oscillations. A pulse width of 200 ns was employed in the tests, and the diode was subjected to a 0.1 per cent duty cycle to minimize possible diode failure due to thermal limitations. Fig. 13 (a) and (b) shows typical operational output waveforms and corresponding power spectrum obtained. Note that pulse – jitter and mode break-up are hardly visible in the waveforms. This result coupled with the symmetry and relatively well-defined nature of the spectrum indicates low – noise, stable trapped-plasma mode oscillations. The diode RF performance capability shown in Fig. 13 (c), compares the theoretical calculations using MWA 729 and the experimental results. As may be easily seen the theory exhibits close correlation with the practice confirming the applicability of the theory to practical design.

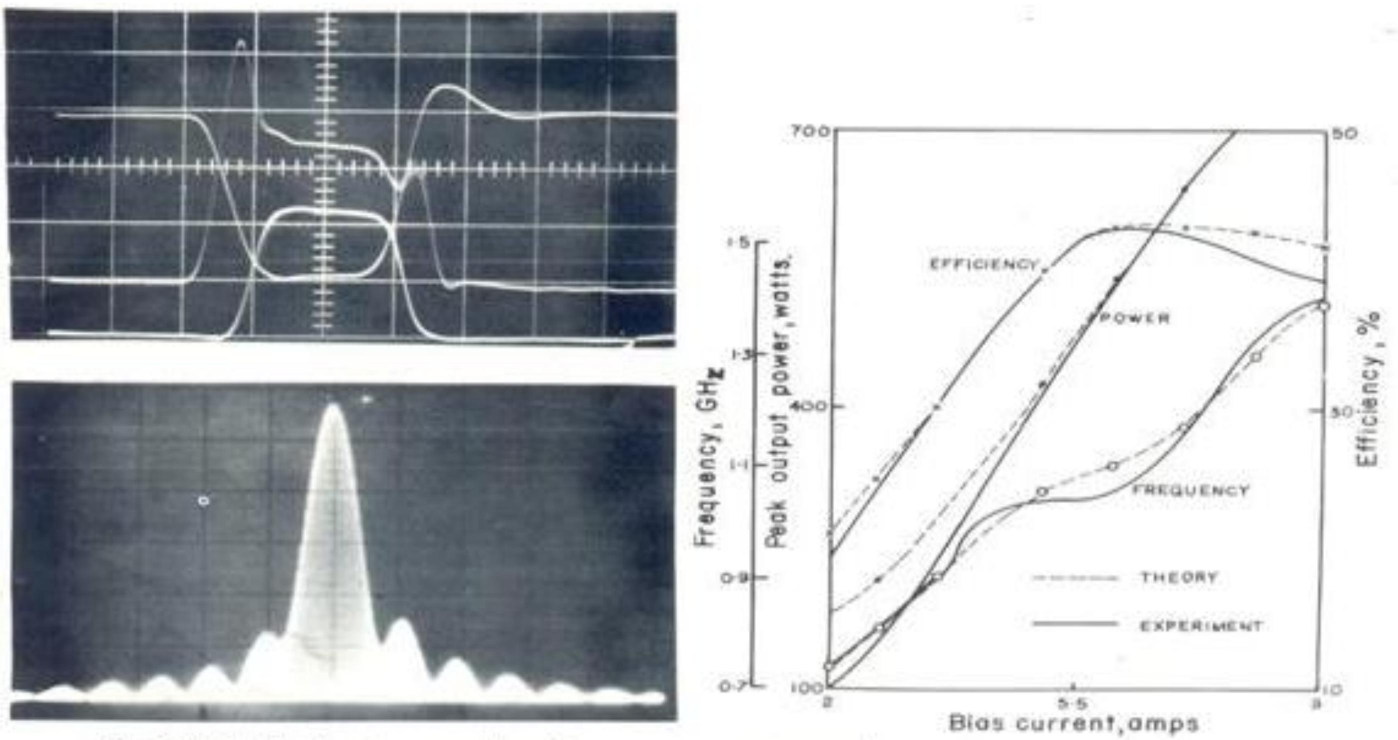

Fig.13(a): Typical operational output waveforms (Top Bias current - 5A/div; Middle Bias voltage - 50v/div; Bottom Detected RF - o.iv/div Horizontal Scale: 200 ns/div.) (b) Corresponding Linear Pulse Spectrum (f_1 = 1.36 GHz, P_1 = 496 watts). (c) R.F. Performance (theory and experiment).

4.0 . CONCLUSIONS

An economical modeling approach that is suitable for the analysis of both the actual TRAPATT device physics and the diode-external circuit interaction has been developed. Results obtained suggest that careful control of diffusion current parameters is essential during TRAPATT diode fabrication. It is shown that, for a given TRAPATT diode structure, the effective avalanching width rather than the nominal active region width could be an important frequency controlling parameter. Although large values of inductance in the vicinity of the diode inductance in the vicinity of the diode may cause amplitude distortion during the high conducting state of the diode, a moderate value of this inductance is shown to be necessary for optimum diode performance.

The present analysis offers a significant advance on previous trapped-plasma oscillations models in giving a more detailed description of the intrinsic diode behaviour, in shedding light on the manner in which the diode package circuit parasitics and diode physical parameters affect the diode performance, in dilineating the useful operating frequency limits of a given diode structure, and finally in providing a relatively simple technique for device-external circuit interaction evaluation. The procedure outline in this work offers opportunities for the designer to rapidly and carefully optimize the diode, and the diode – external circuit interaction, can be readily applied to the modeling of other semi-conductor devices, and provides an excellent basis for the fuller exploitation of the potential system applications of high power, high efficiency semiconductor devices.

ACKNOWLEDGEMENT

The author wishes to express his gratitude to the Silicon Devices processing section of the Semiconductor Device and Components Department, Hughes Aircraft Company, Torrance, California for their collaboration, and to his colleagues of the Electronics and Communications Group for their encouragement and useful discussions.

REFERENCE

1. LEE,. C.A. etal, Ionization rates of holes and electrons in silicon, Phys. Rev. 137, A -761, 1964, pp.761-773

2. SZE, S.M., Physics of Semiconductors, John Wiley & Sons, 1969, pp.60-61.

3. Ibid, pp. 58-59

4. DUH, C.Y. and MOU, J.L., Electron drift velocity in avalanching silicon diodes, IEEE Trans. Elect. Devices, ED – 14, 1967,pp.38.

5. OBAH, C.O.G. etal, Single-diode 0.5kw TRAPATT oscillator, Electronics letters, Vol. 10, No.21, October 1974, pp. 430-431

6. OBAH, C.O.G. 1KW single diode TRAPATT oscillator-fabrication and performance characteristics, PEM Seminar H.A.C., C.A., November 1976, Cont. No. DAABOS – 73-C-2070.

7. CLOFEINE, A.S. etaal, Lumped-element high power TRAPATT circuits, RCA Rev. Vol. 34, 1973, pp. 580-594

8. OBAH, C.O.G. etal, High-power pulsed UHF and L-band p^+ -n $-n^+$ silicon TRAPATT diode oscillators, IEEE Trans. Microwave Th. & Tech., Vol. MTT 23, No. 12 (Special Issue) 1975, pp. 959-970.

9. REYNOLDS, J.F. etal, A solid – state transponder source using high-efficiency silicon avalanche oscillators, RCA Rev., Vol. 33,1972, pp. 344-356.

10. WILSON, W.E., pulsed LSA and TRAPATT sources for microwave systems, Microwave J., August 1971, pp, 33-41

11. ROSEN, A. etal, Widel – and class – C TRAPATT amplifiers, RCA Rev., Vol. 33, 1972, pp. 759-736.

12. OBAH, C.O.G. etal, PEM, Solid state oscillators for fuses, Tech. Report Hughes Aircraft Co., July 1976, Cont. No. DAABOS-75-C-120p.

13. SCHARFETTER, D.L., Power-frequency characteristics of the TRAPATT diode mode in high efficiency power generation in germanium and silicon avalanche diodes, Bell Syst. Tech. J., May-June 1970, pp. 799-826.

14. CLORFEINE, A.S. etal, A theory of high efficiency mode oscillation in avalanche diodes, RCA Rev., September 1969, pp. 397-421.

15. SCHARFETTER, D..L etal, Large signal analysis of a silicon Read diode oscillator, IEEE Trans. Elect. Devices, Vol. ED – 16, 1969, pp. 64-77.

16. HACHTEL, G.D. etal, A new efficient one – dimensional analysis program for junction device modeling, Proc. IEEE (Special Issue on COMPD) Vol. 60, 1972, pp. 86 - 98

17. CARROLL, J.E. etal A computer simulation of TRAPATT circuit, Int. J. of Electronics, Vol. 32, No. 3, 1972, pp. 273-296.

18. EVANS, W.J. etal, characteristics of avalanche diode TRAPATT oscillators, IEEE Trans. Elect. Dev., Vol. ED- 17, 1970, pp 397-404.

19. MONROE, J.W., The effects of package parasitics on the stabiliy of microwave negative resistance devices, IEEE Trans. Microwave Th. & Tech. MTT – 21, 1973 pp. 668-780.

20. GETSINGER, W.J.,The packaged and mounted diode as a microwave circuit, Ibid MTT-14,1966, pp. 56-69.

21. EVANS, W.J. circuits for High – efficiency Avalanche Diode Oscillators, IEEE Trans. Microwave Th. Tech.., Vol. MTT – 17, No. 12 1969, pp. 1060-1067.